

## Article

# An Investigation into the Adsorption of Ammonium by Zeolite-Magnetite Composites

Xiaoming Huang<sup>1,2</sup>, Ning Wang<sup>1</sup>, Zhang Kang<sup>1</sup>, Xiao Yang<sup>1</sup> and Min Pan<sup>1,3,\*</sup>

<sup>1</sup> Fujian Engineering and Research Center of Rural Sewage Treatment and Water Safety, School of Environmental Science and Engineering, Xiamen University of Technology, Xiamen 361024, China; huangxm@xmut.edu.cn (X.H.); 2022031264@s.xmut.edu.cn (N.W.); 1911601115@s.xmut.edu.cn (Z.K.); 1911601132@s.xmut.edu.cn (X.Y.)

<sup>2</sup> Key Laboratory of Water Resources Utilization and Protection of Xiamen, Xiamen University of Technology, Xiamen 361024, China

<sup>3</sup> Laboratory of Environmental Biotechnology (XMUT), Fujian Province University, Xiamen 361024, China

\* Correspondence: panmin@xmut.edu.cn; Tel.: +86-592-6291138

**Abstract:** The discharging of ammonium from industrial, domestic, and livestock sewage has caused eutrophication of the water environment. The objectives of this study are to synthesize magnetic zeolite (M-Zeo) by an eco-friendly, economical, and easy procedure and to investigate its suitability as an adsorbent to remove ammonium from an aqueous solution. Based on characterization from XRD, BET, and SEM-EDS, Fe<sub>3</sub>O<sub>4</sub> was proved to successfully load on natural zeolite. The effect of pH, temperatures, reacting times, initial ammonium concentrations, and regeneration cycles on ammonium adsorption was examined by batch experiments. The ammonium adsorption process can be best described by the Freundlich isotherm and the maximum adsorptive capacity of 172.41 mg/g was obtained. Kinetic analysis demonstrated that the pseudo-second-order kinetic model gave the best description on the adsorption. The value of pH is a key factor and the maximum adsorption capacity was obtained at pH 8. By using a rapid sodium chloride regeneration method, the regeneration ratio was up to 97.03% after five regeneration cycles, suggesting that M-Zeo can be recycled and magnetically recovered. Thus, the economic-efficient, great ammonium affinity, and excellent regeneration characteristics of M-Zeo had an extensively promising utilization on ammonium treatment from liquid.

**Keywords:** ammonium; clinoptilolite; adsorption capacity; magnetic recovery



**Citation:** Huang, X.; Wang, N.; Kang, Z.; Yang, X.; Pan, M. An Investigation into the Adsorption of Ammonium by Zeolite-Magnetite Composites. *Minerals* **2022**, *12*, 256. <https://doi.org/10.3390/min12020256>

Academic Editors: Francisco Franco and Nikolaos Kantiranis

Received: 8 December 2021

Accepted: 11 February 2022

Published: 17 February 2022

**Publisher's Note:** MDPI stays neutral with regard to jurisdictional claims in published maps and institutional affiliations.



**Copyright:** © 2022 by the authors. Licensee MDPI, Basel, Switzerland. This article is an open access article distributed under the terms and conditions of the Creative Commons Attribution (CC BY) license (<https://creativecommons.org/licenses/by/4.0/>).

## 1. Introduction

Nitrogen compounds, ammonium or ammonia generated from population growth, agriculture, and food predicting, in particular, in sufficient concentration can promote water eutrophication. The presence of ammonium in industrial, domestic, and livestock sewage has always been a major concern. The increasing amount of ammonium in wastewater requires efficient sewage treatment technologies, including air stripping, biological treatment, electrochemical treatment, membrane distillation, struvite precipitation, microwave radiation, absorption, and ion exchange [1–4]. Biological treatment is considered the most efficient method on ammonium removal from wastewater with high nitrogen concentration. However, the traditional steps for ammonium removal in biological treatment comprise aerobic nitrification and anoxic denitrification, which consumes abundant energy [5,6]. In addition, large structure floor area, sensitive to shock load, high capital investment and operation cost, and complex management limit its large-scale practical application. More importantly, the current sewage treatment system cannot eliminate the strong disturbance of human activities to the nitrogen compounds in the natural process, and still lead to many nitrogen compounds finally discharged into the water environment. Actually, ammonium or ammonia is also a resource and should be recovered from wastewater. Dawson

and Hilton (2011) reported that about 0.9% of the world's energy is consumed on the production of nitrogen fertilizers [7]. Thus, the growing need of nitrogen may be solved by recovering ammonium from wastewater. Due to adsorbents that are required to have great physical and chemical properties, and also taking the technical, economical, and health-related points into consideration, the technology of adsorption shows great potential for ammonium recovered from wastewater [8].

Zeolite, with regular nanoporous structures, is mainly composed of aluminosilicates with a three-dimensional structural composed by Al-O and Si-O tetrahedra networks [3,9]. Zeolite has an excellent ion exchange capacity, and its cation exchange ranking is  $\text{Cs}^+ > \text{Rb}^+ > \text{K}^+ > \text{NH}_4^+ > \text{Sr}^+ > \text{Na}^+ > \text{Ca}^{2+} > \text{Fe}^{3+}$  [10,11]. Its mineral framework comprises many openings, internal voids, or channels, which are beneficial to trap and bind ammonium [12]. Comparing with other adsorbents for ammonium removal, for example, clay minerals, activated carbon, exfoliated vermiculites, fly ash, peats, chitosan beads, wood sawdust, bentonite, attapulgite, oxide nanoparticles, and zero-valent iron, with disadvantages of complex preparation, high cost, or challenging for low concentration of ammonium removal, natural zeolite has great advantages, being of low cost and easy to obtain, having a high cationic exchange property, and is environment friendly, which allows zeolite as a particular attractive cation exchanger and adsorbent to capture ammonium from wastewater [13]. In addition, zeolite has always been drawing extensive interests on ammonium removal in different ways, for example, ion exchange columns, catalyst, fillers in membrane, and fillers or carriers in biological reactors [14–22]. However, comparing with natural zeolite, modified zeolite exhibits larger adsorptive capacities and higher selectivity for ammonium [1]. In general, common modification techniques for zeolite involve acid treatment, alkali treatment, salty treatment, heat treatment, electrochemical method, and microwave treatment [4,10,11,23–28]. In fact, powder adsorbents have tremendous and attractive advantages on specific surface area and adsorption capacity. Unfortunately, the difficulty in separating powder adsorbents from liquid causes many engineering problems and limits its practical application, for example, the mass loss will flow, blockage, or damage the following treatment structures, and the adsorption capacity reduced by microorganisms, etc. Thus, powder zeolites are also trapped into a dilemma to remove ammonium from real sewage. Recently, the appearance of magnetic materials solves those problems. The powdered magnetic modified adsorbent can be separated by magnetic recovery technology after the adsorption of pollutants and then reused by regeneration. Magnetic materials have been proven to have higher surface area, greater adsorption capacity, and magnetic separation properties [29]. Thus, the preparation of magnetic zeolite may have advantages in the ammonium treatment process. However, magnetic zeolite is commonly used for refinery oily wastewater purification [30], heavy crude oil removal [31], and heavy metal removals [32], etc.

The purposes of this research are to synthesize magnetic zeolite (M-Zeo) and to systematically examine its application on the ammonium removal from aqueous solutions. The effect of pH, temperatures, reacting times, initial ammonium concentrations, and regeneration cycles on ammonium adsorption were investigated by batch experiments. The adsorption isotherms, thermodynamic parameters, and kinetic models were used to discuss the adsorption mechanism of ammonium on M-Zeo.

## 2. Materials and Methods

### 2.1. Materials

The natural zeolite powder (N-Zeo) (<200 mesh) utilized in this experiment was gained from Xuancheng, Anhui province of China. The preparation method followed Mu et al. [33].  $\text{FeCl}_3$  (2 g) was dispersed into ethylene glycol solution (60 mL), then, polyethylene glycol (1.2 g) and sodium acetate (4.8 g) were dissolved into the solution. After stirring for 30 min, 0.8 g natural zeolite (N-Zeo) was added to the mixture and ultrasonicated for 3 h. After that, the mixture was put into a polytetrafluoroethylene-lined autoclave (100 mL) and heated at 190 °C for 8 h. The black composite after cooling to ambient temperature was bathed

by using ethanol and deionized water for a few times until the conductivity was below  $10 \mu\text{S}/\text{cm}$ . The M-Zeo was obtained after drying at  $40^\circ\text{C}$  for 24 h.

Except zeolite, other reagents (such as ferric chloride, ammonium chloride, ethylene glycol, and so on) employed in the current contribution were all of an analytical reagent and purchased from Sinopharm Chemical Reagent Co., Ltd. (Shanghai, China).

## 2.2. Batch Adsorption Experiments

The influence of pH on the ammonium adsorptive capacity by M-Zeo was tested under ambient conditions.  $\text{NH}_4^+\text{-N}$  solutions (50 mL, 1000 mg/L) were put into 100 mL polyethylene centrifuge tubes with caps, then, the pH value was regulated to 4, 5, 6, 7, 8, and 9 by using 1M HCl or 1M NaOH solutions. A total of 0.02 g adsorbent (M-Zeo) was respectively added into  $\text{NH}_4^+\text{-N}$  solutions and then mingled in thermostatic shakers for 12 h (200 rpm,  $25^\circ\text{C}$ ). After equilibrium, the solid phase was separated from the liquid phase by centrifuging, filtering (membrane filter,  $0.45 \mu\text{m}$ ), or magnetic attraction, and then  $\text{NH}_4^+\text{-N}$  concentrations were tested.

$\text{NH}_4^+\text{-N}$  adsorption isotherms were performed in thermostatic shakers for 12 h at the desired temperatures (298 K, 308 K, and 318 K). A total of 0.02 g adsorbent (M-Zeo) was respectively added into the  $\text{NH}_4^+\text{-N}$  solutions (50 mL) at pH = 8 and initial concentrations at a range from 5 to 1000 mg/L (5, 50, 100, 200, 500, and 1000 mg/L).

The kinetics adsorption was evaluated at pH = 8 and at 298 K. A total of 0.02 g adsorbent (M-Zeo) were adopted into  $\text{NH}_4^+\text{-N}$  solutions (50 mL, 1000 mg/L). Samples were withdrawn at continuous intervals (0.25, 0.5, 1, 2, 4, 8, and 12 h).

The impact of the regeneration cycles on the adsorption capacity of ammonium was performed at pH=8 and at 298 K. The adsorbents after adsorption were collected and regenerated by using NaCl solutions (50 mL, 2 mol/L). After washing with deionized water for a few sequences, the regenerated M-Zeo was dried at  $60^\circ\text{C}$  for 24 h and then reused to adsorb ammonium from the aqueous solution.

## 2.3. Analysis Methods

The  $\text{NH}_4^+\text{-N}$  concentrations were analyzed by the Nessler's reagent spectrophotometry method with a spectrophotometer (722E, Spectrum Co., Shanghai, China). The mineral phases were performed by X-ray diffraction (XRD) analysis using an X-Ray diffractometer (SmartLab, Rigaku, Japan) with a Cu-target and a range of  $5\text{--}70^\circ$  at a scan rate of  $10^\circ \text{min}^{-1}$ . The morphology and nanostructures of M-Zeo were analyzed by a field emission scanning electron microscope (FESEM, Sigma 300, Zeiss Ltd., Cambridge, UK) with an electron acceleration voltage of 10 kV. The analysis of surface area and pore circumstances of M-Zeo were performed by using a surface area and pore size analyzer (Quanta NOVA 3000e, Quantachrome, Shanghai, China).

## 3. Results

### 3.1. Characterization

Figure 1 illustrates the XRD patterns of N-Zeo and M-Zeo. The characteristic diffraction peaks of clinoptilolite appeared on  $2\theta = 9.76, 11.16, 22.36, 28.04, 30.02,$  and  $31.92^\circ$ . The reflection at  $2\theta = 26.56^\circ$  was found and authenticated as quartz according to the standard database. Clinoptilolite was the main phase coexisting with quartz in adsorbents, but the intensities of quartz and clinoptilolite superficially became weaker after modification. As a matter of fact, the diffraction patterns at  $2\theta = 35.42, 57.28,$  and  $62.48^\circ$  identified as magnetite show strong diffraction peaks in the sample of M-Zeo, which proved magnetite as a new phase successfully loaded on zeolite.

The SEM images of adsorbents used in the present study are presented in Figure 2. Plate-like morphology crystals, flat surfaces, and massive pores of the zeolite and the channels inside of the zeolite framework can be observed in Figure 2a. Many  $\text{Fe}_3\text{O}_4$  particles with a scale of 200–300 nm were loaded on the surface of zeolite after magnetic

modification in Figure 2b. The EDS analysis (Figure 2c) also proved that the surface of zeolite was coated with plenty of magnetite.

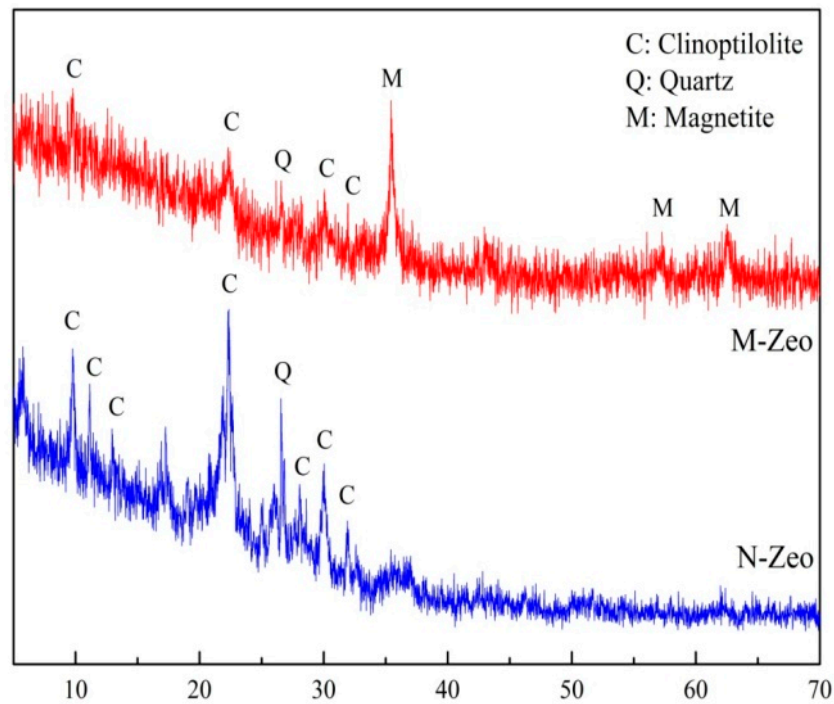
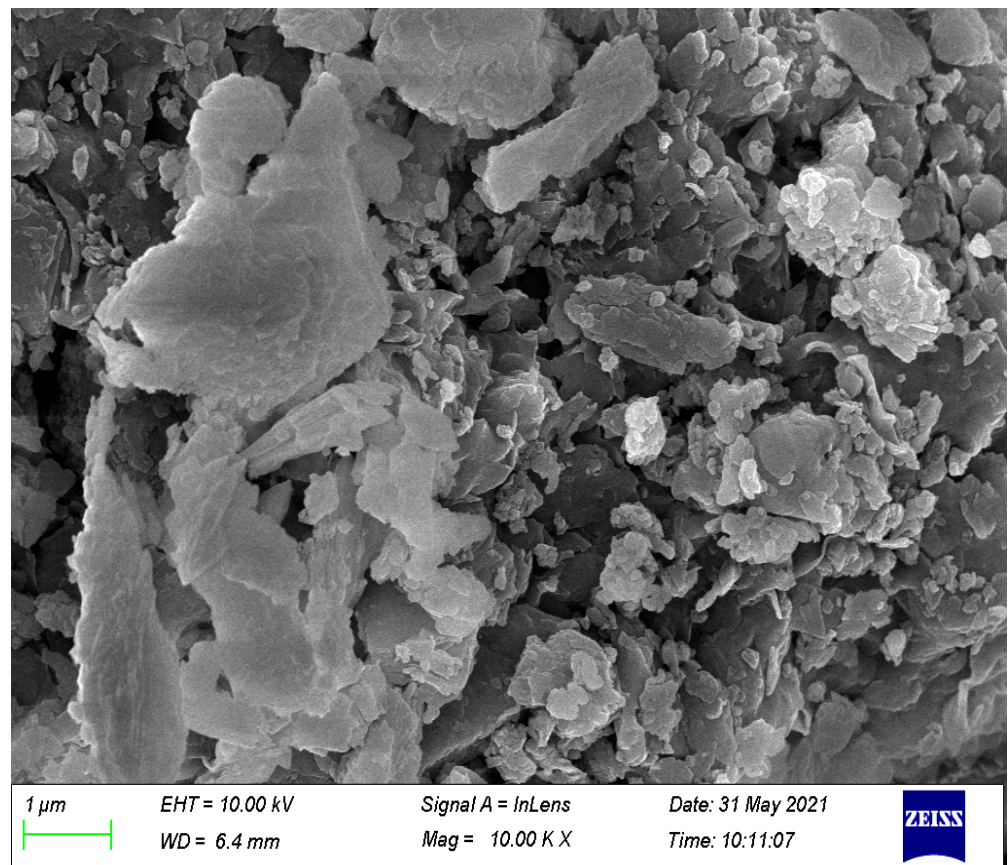
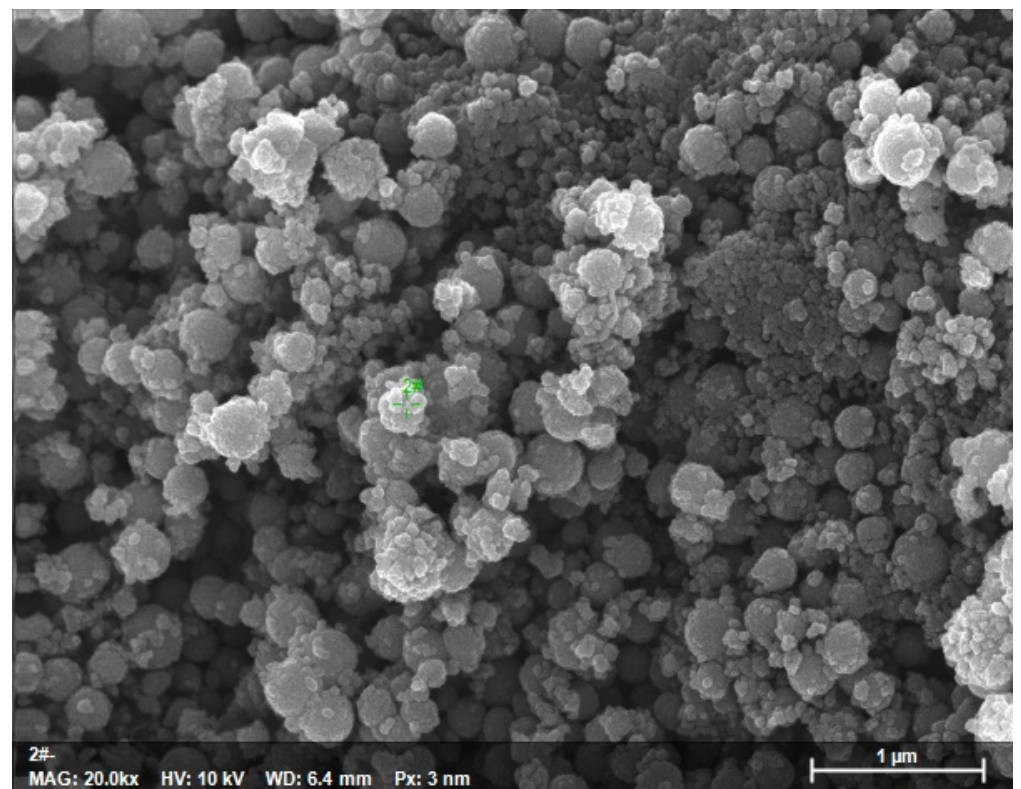


Figure 1. XRD patterns of the N-Zeo and M-Zeo.

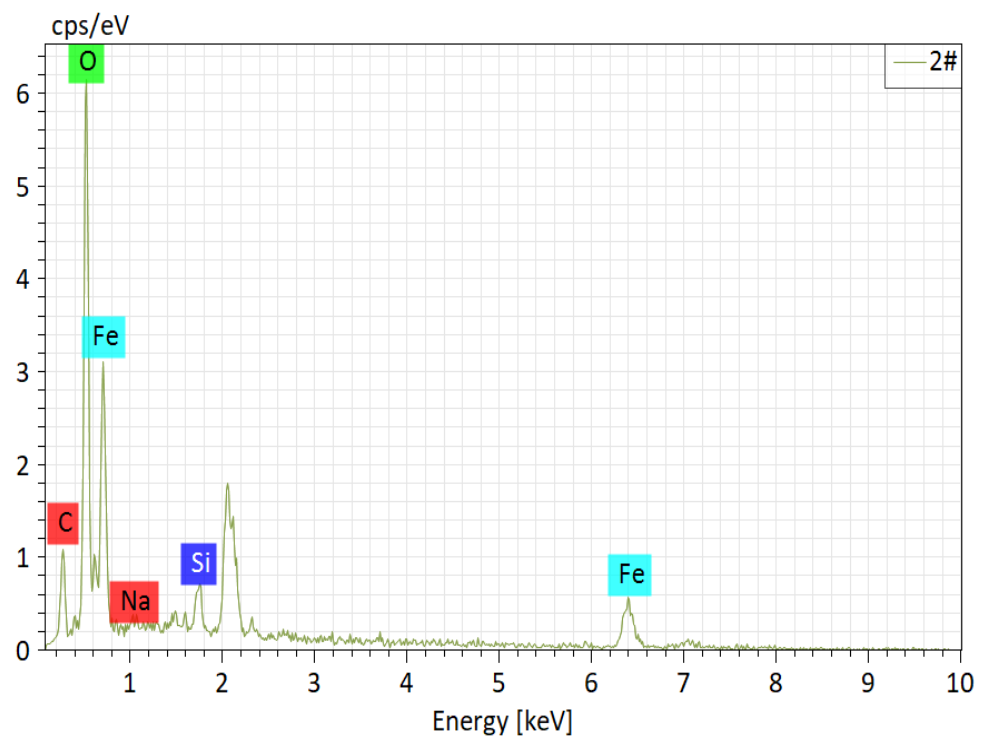


(a)

Figure 2. Cont.



(b)



(c)

**Figure 2.** SEM images of N-Zeo (a), M-Zeo (b), and EDS of M-Zeo (c).

The BET-specific surface area, pore volume, and pore size are templated in Table 1. M-Zeo had better BET-specific surface area and pore volume than N-Zeo. The increase in BET of M-Zeo was attributed to the nanoscale of magnetite occupied on the surface of zeolite.

The adsorption curves of both N-Zeo and M-Zeo showed a shape of IV isotherm (Figure 3), implying the characteristic feature of mesoporous materials. Thus, these mesoporous materials provide more internal specific surface and pore volume [34].

**Table 1.** The values of specific surface area, pore volume, and average pore size of N-Zeo and M-Zeo.

Sample	BET (m <sup>2</sup> /g)	Volume (cc/g)	Pore Size (nm)
N-Zeo	21.283	0.074	69.371
M-Zeo	43.097	0.138	63.814

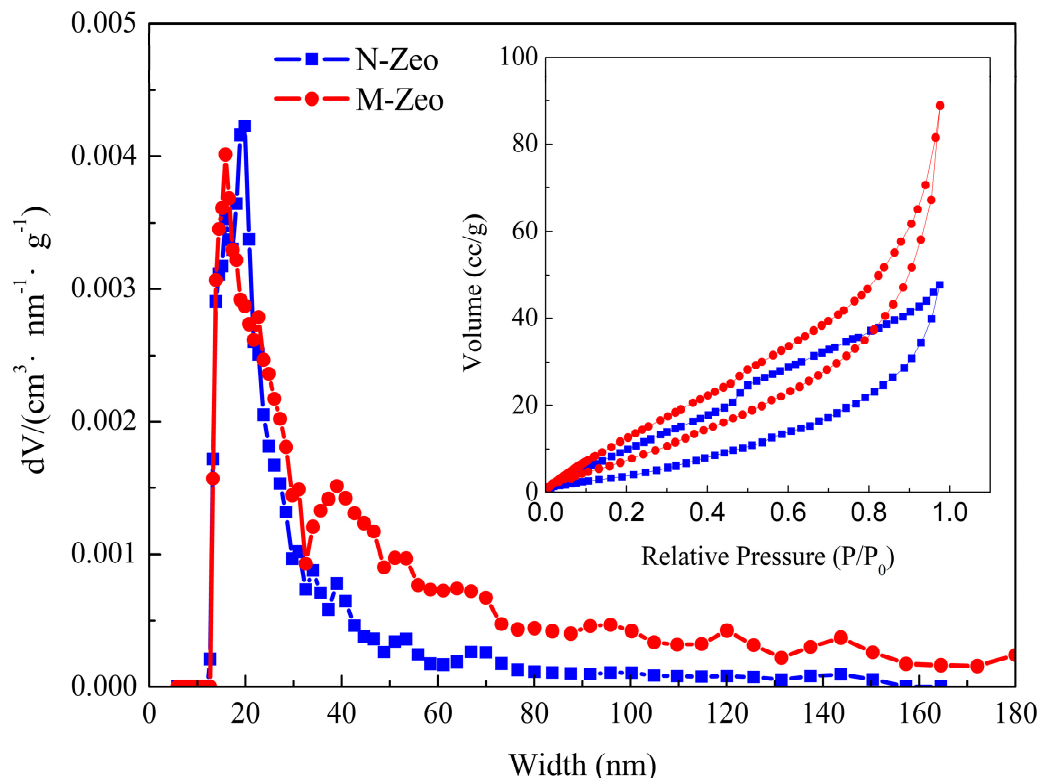


**Figure 3.** N<sub>2</sub> adsorption–desorption isotherms and pore size distributions.

### 3.2. Influence of pH on Ammonium Removal

The impact of pH values on NH<sub>4</sub><sup>+</sup>-N adsorption by using M-Zeo as an adsorbent was performed by adjusting pH values in a range from 4.0 to 9.0. As shown in Figure 4, among the initial pH values, the maximum ammonium adsorption takes place at pH 8.0. The results proved that the adsorption process in the current study was pH-dependent. The adsorption capacity of ammonium clearly rose from 73.84 mg/g to 140.97 mg/g in the pH range from 4.0–8.0, and then declined to 115.94 mg/g at pH 9.0. The present study observed the same trend in a pH rise with other literatures [11,27,35]. The balance between NH<sub>3</sub> and NH<sub>4</sub><sup>+</sup> is pH and temperature-dependent, and the relationship between ammonium and ammonia in an aqueous solution can be expressed as follows:

$$[NH_3] = \frac{[NH_3 + NH_4^+]}{1 + [H^+]/Ka} \tag{1}$$

$$pKa = 4 \times 10^{-8} \times T^3 + 9 \times 10^{-5} \times T^2 - 0.0356 \times T + 10.072 \tag{2}$$

where [NH<sub>3</sub>], [NH<sub>3</sub> + NH<sub>4</sub><sup>+</sup>], and [H<sup>+</sup>] are expressed as the concentrations of NH<sub>3</sub>, NH<sub>3</sub> + NH<sub>4</sub><sup>+</sup>, and H<sup>+</sup> in an aqueous solution, respectively. Ka is the acid ionization constant for ammonia, which was 5.39 × 10<sup>-8</sup> L/mol obtained by Campo et al. [36]. pKa can be stated in a temperature relation formula (°C), represented in Equation (2). Therefore, pKa was calculated

as 9.24 according to the following Equation (2). This was in accordance with ammonium existing as  $\text{NH}_4^+$  at pH 2–8 and  $\text{NH}_3$  at pH 10–13 in the aqueous solution (Figure 4b). At a lower pH, zeolite is highly selective for  $\text{H}^+$  and  $\text{NH}_4^+$  and could be favorable for adsorbing  $\text{NH}_4^+$  on the external surface of the zeolite. At a higher pH, the decrease of ammonium adsorption capacity can be attributed to the alkaline condition promoting  $\text{NH}_4^+$  turning into  $\text{NH}_3$ .

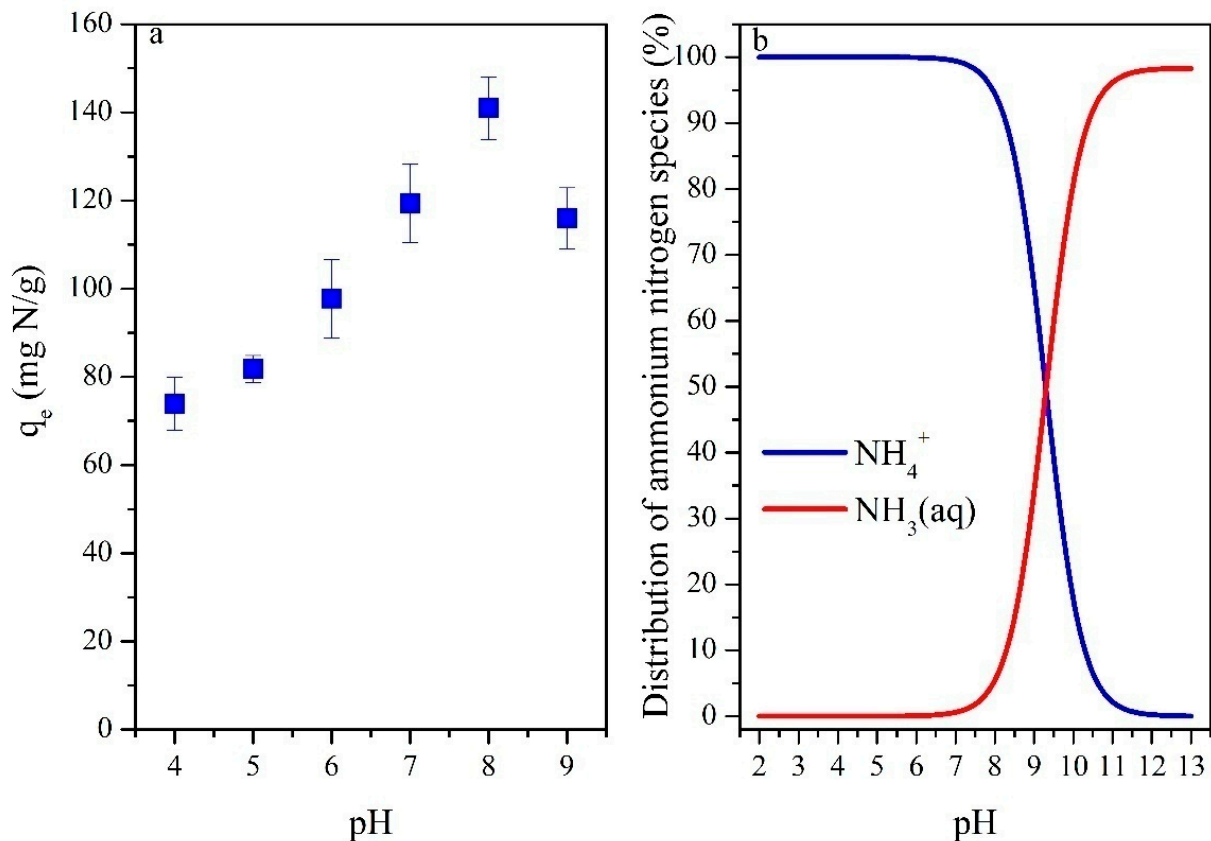


**Figure 4.** (a) Impact of pH on  $\text{NH}_4^+$ -N removal efficiency from liquid by using M-Zeo as adsorbent; (b) distribution of ammonium species in liquid.

### 3.3. Adsorption Isotherms and Thermodynamics

Three adsorption models of the Langmuir model, the Freundlich model, and the D-R isotherm were used to fit the process of the M-Zeo adsorbing ammonium [37–39]. The Langmuir model is described as Equation (3):

$$\frac{C_e}{q_e} = \frac{1}{q_m} C_e + \frac{1}{q_m k} \quad (3)$$

here,  $q_m$  is the maximum adsorptive capacity (mg/g);  $k$  (L/mg) refers to the Langmuir constant;  $C_e$  is the equilibrium concentration (mg/L);  $q_e$  is the adsorption capacity on adsorbent (mg/g).

The Freundlich model is represented as Equation (4):

$$\ln q_e = \ln K_f + \frac{1}{n} \ln C_e \quad (4)$$

here,  $K_f$  (mg/g) refers to the Freundlich constant.  $1/n$  is a heterogeneous factor, which is involved in the adsorption intensity or surface heterogeneity.

The D-R isotherm is given as Equation (5):

$$\ln q_e = \ln q_m - \beta \epsilon^2 \tag{5}$$

here,  $\beta$  is the adsorption energy constant ( $\text{mol}^2/\text{J}^2$ );  $\epsilon$  is Polanyi potential, which can be calculated as Equation (6):

$$\epsilon = RT \ln\left(1 + \frac{1}{C_e}\right) \tag{6}$$

and  $E$  is the average energy of adsorption (kJ/mol), which is expressed from  $\beta$  in the following Equation (7):

$$E = \frac{1}{\sqrt{2\beta}} \tag{7}$$

The adsorption isotherms under various temperatures are illustrated in Figure 5a. Table 2 shows relative parameters and correlation coefficients summarized from three adsorption isotherm models. The highest values of correlation coefficients  $R^2$  ( $>0.9928$ ) were obtained by fitting with the Freundlich model, indicating that the adsorption was taking place on a structurally heterogeneous adsorbent surface. In this study, the value of the heterogeneous factor  $1/n$  is between 0.4667 and 0.4739 ( $<0.5$ ), which suggests a favorable adsorption in the present research [40]. Further, the maximum adsorption capacity of 172.41 mg/g was obtained from the Langmuir model at 298 K. Based on D-R isotherm, the process of ammonium adsorption could be related to a pore volume filling process [39]. The point of  $E$  distinguishes the class of sorption. Thus, physical sorption is determined by the  $E$  values in the range from 1 to 8 kJ/mol, while chemical sorption is determined by the  $E$  values in the range from 8 to 16 kJ/mol.  $E$  values obtained in present study ranged in 8.9087–9.6225 kJ/mol, demonstrating that the adsorption was predominantly chemisorption.

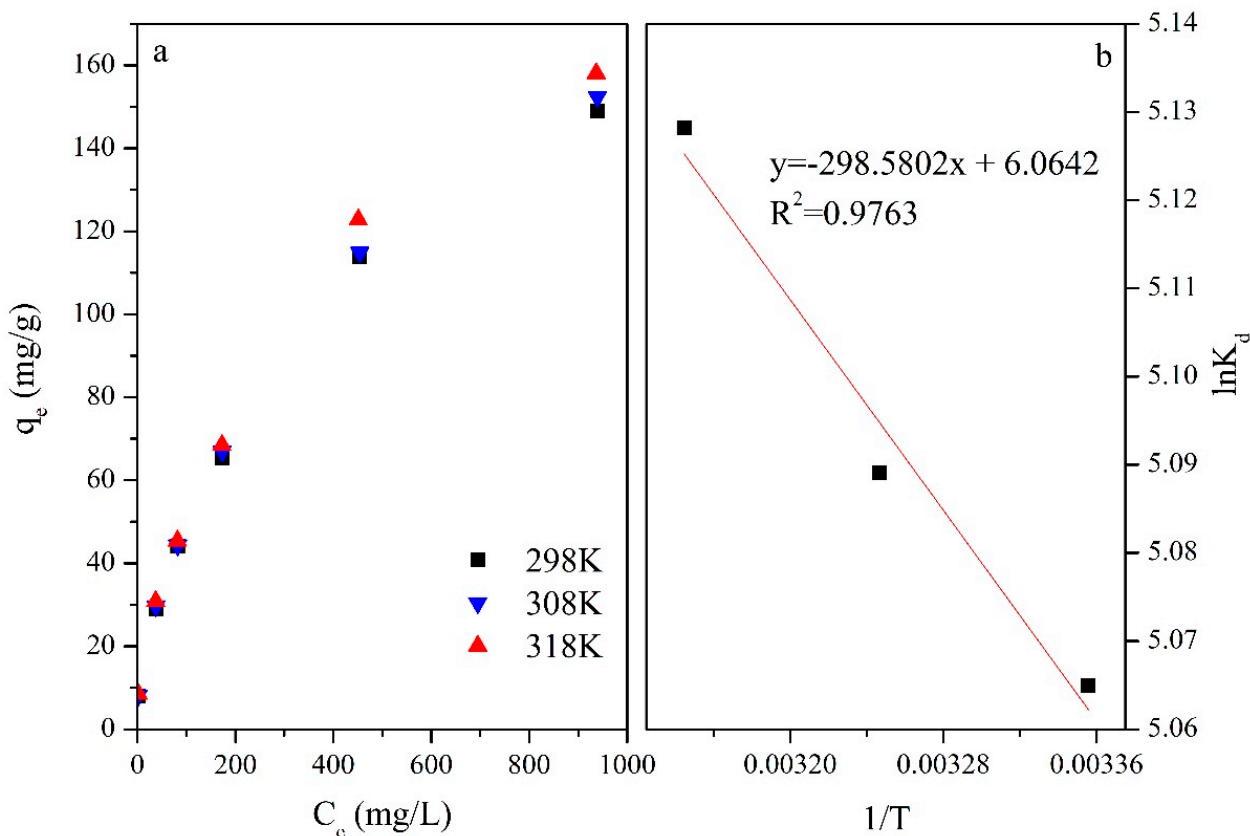


Figure 5. (a) Adsorption isotherms of ammonium on M-Zeo under different temperatures; (b) plots of  $\ln K_d$  vs.  $1/T$ .

**Table 2.** Relative parameters of adsorption isotherms models.

T (K)	Langmuir			Freundlich			D-R			
	$q_m$ (mg/g)	$k$	$R^2$	$K_f$ (mg/g)	$1/n$	$R^2$	$B$ (mol <sup>2</sup> /J <sup>2</sup> )	$q_m$ (mg/g)	$E$ (kJ/mol)	$R^2$
298	172.41	0.005	0.9442	5.73	0.4739	0.9953	0.0063	152.32	8.9087	0.9486
308	175.44	0.005	0.9425	5.92	0.4714	0.9952	0.0059	154.02	9.2057	0.9472
318	181.82	0.005	0.9410	6.33	0.4667	0.9928	0.0054	158.03	9.6225	0.9410

The maximum adsorption capacity in the present study was obviously higher than in other literature. For example, the ammonium exchange capacity by high silica zeolites was 4.08 mg/g [5]. Fu et al. [27] obtained the maximum adsorption amount of ammonium of 16.96 mg/g by using zeolite modified with sodium nitrate (NaNO<sub>3</sub>). Kamyab and Williams [12] reported that the maximum adsorptive amount of ammonium by Linde Type J zeolite was 51.97 mg/g. Meanwhile, Shabanet al. [41] found that the adsorption capacities of ammonium by clinoptilolite and synthetic zeolite-A were, respectively, 92 mg/g and 99 mg/g. Considering the differences, the main reason may be that the nano magnetic particles enhanced the BET specific surface area and pore volume of the adsorbent (Table 2), which promoted greater adsorption ability for the ammonium. Moreover, Vaičiukynienė et al. [42] stated that the increasing initial ammonium concentration encouraged the internal micropores of the adsorbent to take part in ammonium exchange, which facilitated the great adsorption capacity obtained.

### 3.4. Thermodynamic Parameters

The distribution coefficient,  $K_d$ , is represented as Equation (8), and the Gibbs free energy, entropy, and enthalpy are calculated by the temperature-dependent adsorption isotherm (Equations (9) and (10)):

$$K_d = \frac{q_e}{C_e} \quad (8)$$

$$\Delta G^0 = -RT \ln K_d \quad (9)$$

$$\ln K_d = -\frac{\Delta H^0}{RT} + \frac{\Delta S^0}{R} \quad (10)$$

Figure 5b tabulated the relationship between  $\ln K_d$  and  $1/T$ , while Table 3 summarized the thermodynamic parameters values. The value of  $\Delta G^0$ , lower than zero, and the value of  $\Delta H^0$ , higher than zero, determined that the adsorption was endothermic, feasible, and spontaneous. The lower values of  $\Delta G^0$  coupled with higher temperature (Table 3), determined that higher temperatures promoted the endothermic adsorption. The values of  $\Delta S^0$  that were higher than zero revealed that the adsorption was randomness increasing.

**Table 3.** Thermodynamic parameters of ammonium adsorption by M-Zeo.

T (K)	$\Delta G^0$ (kJ/mol)	$\Delta S^0$ (kJ/mol/K)	$\Delta H^0$ (kJ/mol)
298	−12.549		
308	−13.032	0.050	2.482
318	−13.558		

### 3.5. Adsorption Kinetics

Four typical kinetic models simulated the adsorption kinetics are expressed as follows [43–46]:

$$\text{Pseudo first-order equation : } \ln(q_e - q_t) = \ln q_e - k_1 t \quad (11)$$

$$\text{Pseudo second-order equation : } \frac{t}{q_t} = \frac{1}{k_2 q_e^2} + \frac{t}{q_e} \quad (12)$$

$$\text{Elovich equation : } q_t = \frac{\ln a_e b_e}{b_e} + \frac{1}{b_e} \ln t \tag{13}$$

$$\text{Intraparticle diffusion equation : } q_t = k_3 t^{0.5} \tag{14}$$

here,  $q_t$  is the amount of adsorption at time  $t$ , mg/g;  $q_e$  is the amount of adsorption at equilibrium, mg/g;  $k_1$  and  $k_2$  are, respectively, the rate constants of pseudo first-order adsorption and pseudo second-order adsorption, g/(mg·h);  $a_e$  is the initial adsorption rate, mg/(g·h);  $b_e$  is described to the extent of surface coverage and the activation energy for chemisorption, g/mg;  $k_3$  is the rate constant of intraparticle diffusion, mg/(g·h<sup>-0.5</sup>).

Figure 6a shows the adsorption kinetics at pH 8. It is observed that the adsorption significantly rose with the increasing contact time after 1 h. The adsorption quantity was 151.22 mg/g at a contact time of 12 h at 298 K. The data of adsorption kinetics stated that M-Zeo presented a fast adsorption rate for ammonium removal.

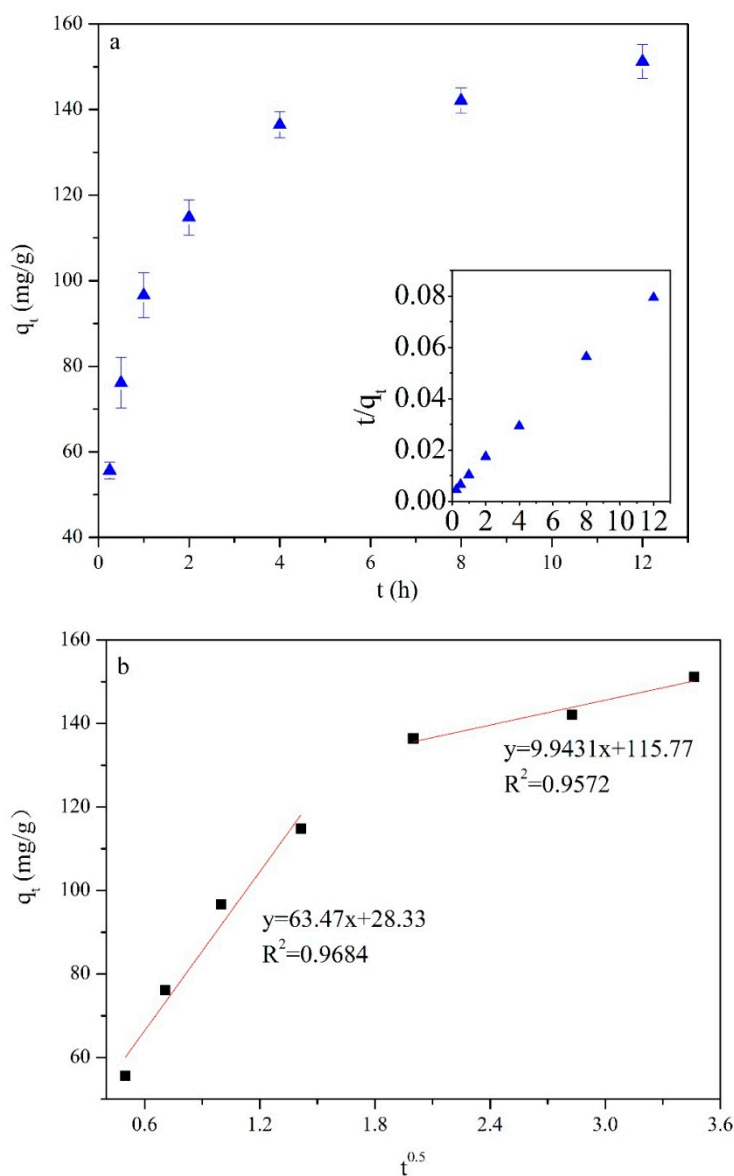


**Figure 6.** (a) Adsorption kinetics of ammonium on M-Zeo and the pseudo-second-order model; (b) the intraparticle diffusion model.

The kinetic parameters after kinetic data in the current study fitted by the above four kinetic models were summarized in Table 4. It is observed that the adsorption kinetic data

can be satisfactorily simulated by a pseudo-second-order model with the highest correlation coefficient  $R^2 = 0.9990$ . According to the pseudo-second-order model, the theoretically adsorbed amount at equilibrium was calculated as 156.25 mg/g, which was close to the value obtained from the experiment (151.22 mg/g). Because of the correlation coefficient  $R^2$  higher than 0.99, the Elovich model acceptably fitted the kinetic data, supposing that the adsorption was energetically heterogeneous [47]. As observed in Figure 6b, the adsorption kinetic data can be satisfactorily simulated by the intraparticle diffusion model if the entire curve is separated into two linear patterns. Therefore, the adsorption can be considered to involve two stages, respectively, corresponding to the boundary layer diffusion and the intraparticle diffusion [11]. The fast stage at the first two hours belonged to the rapid occupation of major surface adsorption positions by ammonium, while the gradual stage is ascribed to ammonium entering the internal pores of M-Zeo by the intraparticle diffusion [10]. Thus, the adsorption is firstly rapid adsorption and then gradual equilibrium.

**Table 4.** Kinetic parameters of ammonium adsorption by M-Zeo.

Kinetic Model	Pseudo First-Order			Pseudo Second-Order			Simple Elovich			Intraparticle Diffusion	
	$q_e$ (mg/g)	$k_1$ ( $h^{-1}$ )	$R^2$	$q_e$ (mg/g)	$k_2$ (g/mg·h)	$R^2$	$a_e$ (mg/(g·h))	$b_e$ (g/mg)	$R^2$	$k_3$ (mg/g·h <sup>0.5</sup> )	$R^2$
M-Zeo	77.339	0.3026	0.9101	156.25	0.0108	0.9990	1105.2	0.04	0.9830	29.941	0.8664

### 3.6. Regeneration

The regeneration of the M-Zeo performance for ammonium adsorption is exhibited in Figure 7. After the second regeneration cycle, the adsorption quantities were clearly increased from 153.49 mg/g to 166.00 mg/g. However, after regeneration by the third cycle, the adsorption quantities were declined. After five regeneration cycles, the adsorption quantity was 148.94 mg/g, with the regeneration ratio of 97.03%. Meanwhile, M-Zeo was proven to have great advantages on magnetic recovery and reused properties by employing the NaCl regeneration method.

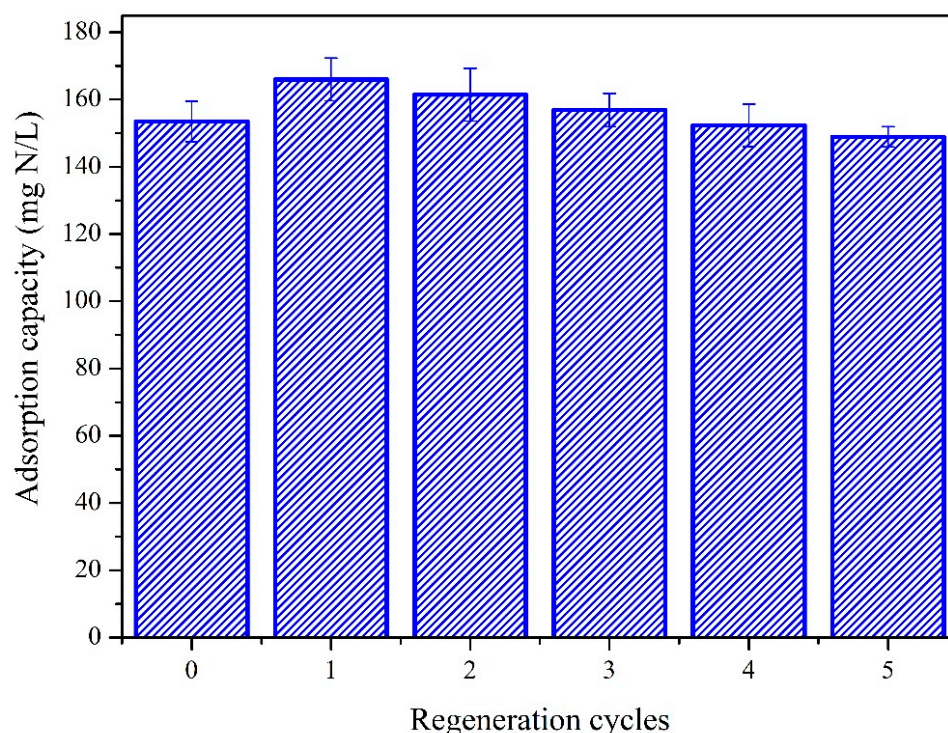
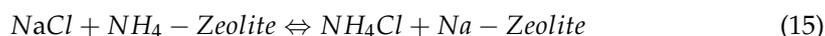


**Figure 7.** The adsorption capacities with regeneration times.

The ion-exchange equilibrium of the process of “NaCl regeneration” of ammonium-bearing zeolite can be expressed as the following [48]:



On the surface of zeolite,  $\text{Na}^+$  exchanged the position of  $\text{NH}_4^+$  and then zeolite recovered the property of ammonium exchanging [49]. Meanwhile, Li et al. [49] proved that after three cycles in NaCl regeneration the adsorbent had the adsorption capacity close to that of fresh zeolite. Thus, NaCl solution can act as both a desorbing agent and regenerating agent, which contributes to  $\text{NH}_4^+$  desorption and M-Zeo regeneration, simultaneously [50].

#### 4. Conclusions

The M-Zeo with high magnetic recovery performance was successfully synthesized. M-Zeo demonstrated a great performance of ammonium removal from liquid. The Freundlich model and the pseudo-second-order model satisfactorily simulated the adsorption isotherm and kinetics for ammonium adsorption on M-Zeo, respectively. The maximum adsorptive capacity of 172.41 mg/g was obtained. The  $E$  values in the range of 8.9087–9.6225 kJ/mol from the D-R model proved that the adsorption process was chemisorption. Thermodynamic parameters determined that the adsorption was endothermic, feasible, and spontaneous. The efficient ammonium removals presented that the economic-efficient, great ammonium affinity, and excellent regeneration characteristics of M-Zeo can be a promising adsorbent extensively utilized in the ammonium treatment of liquid.

**Author Contributions:** M.P. conceived and designed the experiments. M.P., N.W., Z.K., X.Y. and X.H. performed the experiments and contributed to the reagents, materials, and analysis. X.H. organized the characterization analysis. M.P. and X.H. contributed to drafting, writing, and editing of the manuscript. All authors have read and agreed to the published version of the manuscript.

**Funding:** This research was funded by the Scientific Climbing Program of Xiamen University of Technology (XPDKQ18031), Educational Research Project from the Education Department of Fujian Province (JAT200466, JAT200476), the Science and Technology Project of Longyan City (2017LY63), and Natural Science Foundation of the Fujian Province (2021J011177).

**Conflicts of Interest:** The authors declare no conflict of interest.

#### References

1. Probst, J.; Outram, J.G.; Couperthwaite, S.J.; Millar, G.J.; Kaparaju, P. Sustainable ammonium recovery from wastewater: Improved synthesis and performance of zeolite N made from kaolin. *Micropor. Mesopor. Mat.* **2021**, *316*, 110918. [[CrossRef](#)]
2. Ulu, F.; Kobya, M. Ammonia removal from wastewater by air stripping and recovery struvite and calcium sulphate precipitations from anesthetic gases manufacturing wastewater. *J. Water Process. Eng.* **2020**, *38*, 101641. [[CrossRef](#)]
3. Xue, R.; Donovan, A.; Zhang, H.; Ma, Y.; Adams, C.; Yang, J.; Hua, B.; Inniss, E.; Eichholz, T.; Shi, H. Simultaneous removal of ammonia and N-nitrosamine precursors from high ammonia water by zeolite and powdered activated carbon. *J. Environ. Sci.* **2018**, *64*, 82–91. [[CrossRef](#)] [[PubMed](#)]
4. Lei, X.; Li, M.; Zhang, Z.; Feng, C.; Bai, W.; Sugiura, N. Electrochemical regeneration of zeolites and the removal of ammonia. *J. Hazard. Mater.* **2009**, *169*, 746–750. [[CrossRef](#)]
5. Doekhi-Bennani, Y.; Leilabady, N.M.; Fu, M.; Rietveld, L.C.; van der Hoek, J.P.; Heijman, S.G.J. Simultaneous removal of ammonium ions and sulfamethoxazole by ozone regenerated high silica zeolites. *Water Res.* **2021**, *188*, 116472. [[CrossRef](#)] [[PubMed](#)]
6. Pan, M.; Hu, Z.; Liu, R.; Zhan, X. Effects of loading rate and aeration on nitrogen removal and  $\text{N}_2\text{O}$  emissions in intermittently aerated sequencing batch reactors treating slaughter house wastewater at 11 °C. *Bioproc. Biosyst. Eng.* **2015**, *38*, 681–689. [[CrossRef](#)]
7. Dawson, C.J.; Hilton, J. Fertiliser availability in a resource-limited world: Production and recycling of nitrogen and phosphorus. *Food Policy* **2011**, *36*, S14–S22. [[CrossRef](#)]
8. Moussavi, G.; Talebi, S.; Farrokhi, M.; Sabouti, R.M. The investigation of mechanism, kinetic and isotherm of ammonia and humic acid co-adsorption onto natural zeolite. *Chem. Eng. J.* **2011**, *171*, 1159–1169. [[CrossRef](#)]
9. Wen, Q.; Di, J.; Jiang, L.; Yu, J.; Xu, R. Zeolite-coated mesh film for efficient oil–water separation. *Chem. Sci.* **2013**, *4*, 591–595. [[CrossRef](#)]
10. Lin, L.; Lei, Z.; Wang, L.; Liu, X.; Zhang, Y.; Wan, C.; Lee, D.-J.; Tay, J.H. Adsorption mechanisms of high-levels of ammonium onto natural and NaCl-modified zeolites. *Sep. Purif. Technol.* **2013**, *103*, 15–20. [[CrossRef](#)]

11. Pan, M.; Zhang, M.; Zou, X.; Zhao, X.; Deng, T.; Chen, T.; Huang, X. The investigation into the adsorption removal of ammonium by natural and modified zeolites: Kinetics, isotherms, and thermodynamics. *Water SA* **2019**, *45*, 648–656. [[CrossRef](#)]
12. Kamyab, S.M.; Williams, C.D. Pure zeolite LTJ synthesis from kaolinite under hydrothermal conditions and its ammonium removal efficiency. *Micropor. Mesopor. Mat.* **2021**, *318*, 111006. [[CrossRef](#)]
13. He, Y.; Lin, H.; Dong, Y.; Liu, Q.; Wang, L. Simultaneous removal of ammonium and phosphate by alkaline-activated and lanthanum-impregnated zeolite. *Chemosphere* **2016**, *164*, 387–395. [[CrossRef](#)] [[PubMed](#)]
14. Chen, J.; Wang, X.; Chen, Z.; Feng, X.; Chen, X. Application of a synthetic zeolite as a storage medium in SBRs to achieve the stable partial nitrification of ammonium. *Env. Sci. Water Res.* **2019**, *5*, 287–295. [[CrossRef](#)]
15. Wijesinghe, D.T.N.; Dassanayake, K.B.; Scales, P.; Sommer, S.G.; Chen, D. Removal of excess nutrients by Australian zeolite during anaerobic digestion of swine manure. *J. Environ. Sci. Health Part A* **2018**, *53*, 362–372. [[CrossRef](#)]
16. Du, L.; Trinh, X.; Chen, Q.; Wang, C.; Liu, S.; Liu, P.; Zhou, Q.; Xu, D.; Wu, Z. Effect of clinoptilolite on ammonia emissions in integrated vertical-flow constructed wetlands (IVCWs) treating swine wastewater. *Ecol. Eng.* **2018**, *122*, 153–158. [[CrossRef](#)]
17. Moghadassi, A.R.; Rajabi, Z.; Hosseini, S.M.; Mohammadi, M. Preparation and characterization of (PVC-Blend-SBR) mixed matrix gas separation membrane filled with zeolite. *Arab. J. Sci. Eng.* **2013**, *39*, 605–614. [[CrossRef](#)]
18. Malekian, R.; Abedi-Koupai, J.; Eslamian, S.S.; Mousavi, S.F.; Abbaspour, K.C.; Afyuni, M. Ion-exchange process for ammonium removal and release using natural Iranian zeolite. *Appl. Clay. Sci.* **2011**, *51*, 323–329. [[CrossRef](#)]
19. Wang, Y.; Lin, F.; Pang, W. Ion exchange of ammonium in natural and synthesized zeolites. *J. Hazard. Mater.* **2008**, *160*, 371–375. [[CrossRef](#)]
20. Almutairi, A.; Weatherley, L.R. Intensification of ammonia removal from waste water in biologically active zeolitic ion exchange columns. *J. Environ. Manag.* **2015**, *160*, 128–138. [[CrossRef](#)]
21. Jabłońska, M.; Król, A.; Kukulka-Zajac, E.; Tarach, K.; Chmielarz, L.; Góra-Marek, K. Zeolite Y modified with palladium as effective catalyst for selective catalytic oxidation of ammonia to nitrogen. *J. Catal.* **2014**, *316*, 36–46. [[CrossRef](#)]
22. Wang, Y.; Song, X.; Xu, Z.; Cao, X.; Song, J.; Huang, W.; Ge, X.; Wang, H. Adsorption of Nitrate and Ammonium from Water Simultaneously Using Composite Adsorbents Constructed with Functionalized Biochar and Modified Zeolite. *Water Air Soil Poll.* **2021**, *232*, 1–19. [[CrossRef](#)]
23. Liu, X.; Xie, W.; Cui, X.; Tan, Z.; Cao, J.; Chen, Y. Clinoptilolite tailored to methane or nitrogen selectivity through different temperature treatment. *Chem. Phys. Lett.* **2018**, *707*, 75–79. [[CrossRef](#)]
24. Esposito, S.; Dell'Agli, G.; Marocco, A.; Bonelli, B.; Allia, P.; Tiberto, P.; Barrera, G.; Manzoli, M.; Arletti, R.; Pansini, M. Magnetic metal-ceramic nanocomposites obtained from cation-exchanged zeolite by heat treatment in reducing atmosphere. *Micropor. Mesopor. Mat.* **2018**, *268*, 131–143. [[CrossRef](#)]
25. Zhan, Y.; Zhang, H.; Lin, J.; Zhang, Z.; Gao, J. Role of zeolite's exchangeable cations in phosphate adsorption onto zirconium-modified zeolite. *J. Mol. Liq.* **2017**, *243*, 624–637. [[CrossRef](#)]
26. Liu, J.; Cheng, X.; Zhang, Y.; Wang, X.; Zou, Q.; Fu, L. Zeolite modification for adsorptive removal of nitrite from aqueous solutions. *Micropor. Mesopor. Mat.* **2017**, *252*, 179–187. [[CrossRef](#)]
27. Fu, H.; Li, Y.; Yu, Z.; Shen, J.; Li, J.; Zhang, M.; Ding, T.; Xu, L.; Lee, S.S. Ammonium removal using a calcined natural zeolite modified with sodium nitrate. *J. Hazard. Mater.* **2020**, *393*, 122481. [[CrossRef](#)]
28. Li, M.; Feng, C.; Zhang, Z.; Lei, X.; Chen, N.; Sugiura, N. Simultaneous regeneration of zeolites and removal of ammonia using an electrochemical method. *Micropor. Mesopor. Mat.* **2010**, *127*, 161–166. [[CrossRef](#)]
29. Pirsra, S.; Asadzadeh, F. Synthesis of Fe<sub>3</sub>O<sub>4</sub>/SiO<sub>2</sub>/Polypyrrole magnetic nanocomposite polymer powder: Investigation of structural properties and ability to purify of edible sea salts. *Adv. Powder Technol.* **2021**, *32*, 1233–1246. [[CrossRef](#)]
30. Hesas, R.H.; Baei, M.S.; Rostami, H.; Gardy, J.; Hassanpour, A. An investigation on the capability of magnetically separable Fe<sub>3</sub>O<sub>4</sub>/mordenite zeolite for refinery oily wastewater purification. *J. Environ. Manag.* **2019**, *241*, 525–534. [[CrossRef](#)]
31. Lin, D.; Feng, X.; Wu, Y.; Ding, B.; Lu, T.; Liu, Y.; Chen, X.; Chen, D.; Yang, C. Insights into the synergy between recyclable magnetic Fe<sub>3</sub>O<sub>4</sub> and zeolite for catalytic aquathermolysis of heavy crude oil. *Appl. Surf. Sci.* **2018**, *456*, 140–146. [[CrossRef](#)]
32. Liu, H.; Peng, S.; Shu, L.; Chen, T.; Bao, T.; Frost, R.L. Magnetic zeolite NaA: Synthesis, characterization based on metakaolin and its application for the removal of Cu<sup>2+</sup>, Pb<sup>2+</sup>. *Chemosphere* **2013**, *91*, 1539–1546. [[CrossRef](#)] [[PubMed](#)]
33. Mu, B.; Wang, Q.; Wang, A. Preparation of magnetic attapulgite nanocomposite for the adsorption of Ag<sup>+</sup> and application for catalytic reduction of 4-nitrophenol. *J. Mater. Chem.* **2013**, *1*, 7083. [[CrossRef](#)]
34. Sun, F.; Liu, H.; Shu, D.; Chen, T.; Chen, D. The Characterization and SCR Performance of Mn-Containing α-Fe<sub>2</sub>O<sub>3</sub> Derived from the Decomposition of Siderite. *Minerals* **2019**, *9*, 393. [[CrossRef](#)]
35. Yusof, A.M.; Keat, L.K.; Ibrahim, Z.; Majid, Z.A.; Nizam, N.A. Kinetic and equilibrium studies of the removal of ammonium ions from aqueous solution by rice husk ash-synthesized zeolite Y and powdered and granulated forms of mordenite. *J. Hazard. Mater.* **2010**, *174*, 380–385. [[CrossRef](#)] [[PubMed](#)]
36. Campos, J.C.; Moura, D.; Costa, A.P.; Yokoyama, L.; Araujo, F.V.; Cammarota, M.C.; Cardillo, L. Evaluation of pH, alkalinity and temperature during air stripping process for ammonia removal from landfill leachate. *J. Environ. Sci. Health A* **2013**, *48*, 1105–1113. [[CrossRef](#)]
37. Langmuir, I. The adsorption of gases on plane surfaces of glass, mica and platinum. *J. Am. Chem. Soc.* **1918**, *40*, 1316–1403. [[CrossRef](#)]
38. Freundlich, H.M.F. Over the adsorption in solution. *J. Phys. Chem.* **1906**, *57*, 385–470.

39. Hu, Q.; Zhang, Z. Application of Dubinin–Radushkevich isotherm model at the solid/solution interface: A theoretical analysis. *J. Mol. Liq.* **2019**, *277*, 646–648. [[CrossRef](#)]
40. Kostić, M.; Radović, M.; Mitrović, J.; Antonijević, M.; Bojić, D.; Petrović, M.; Bojić, A. Using xanthated *Lagenaria vulgaris* shell biosorbent for removal of Pb(II) ions from wastewater. *J. Iran. Chem. Soc.* **2013**, *11*, 565–578. [[CrossRef](#)]
41. Shaban, M.; AbuKhadra, M.R.; Nasief, F.M.; AbdEl-Salam, H.M. Removal of ammonia from aqueous solutions, ground water, and wastewater using mechanically activated clinoptilolite and synthetic zeolite-A: Kinetic and equilibrium studies. *Water Air Soil Poll.* **2017**, *228*, 1–16. [[CrossRef](#)]
42. Vaiciukyniene, D.; Mikelioniene, A.; Baltusnikas, A.; Kantautas, A.; Radzevicius, A. Removal of ammonium ion from aqueous solutions by using unmodified and H<sub>2</sub>O<sub>2</sub>-modified zeolitic waste. *Sci. Rep.* **2020**, *10*, 352. [[CrossRef](#)] [[PubMed](#)]
43. Lagergren, S. About the theory of so-called adsorption of soluble substances. *Sven. Vetén. Hand.* **1898**, *24*, 1–39.
44. Ho, Y.S.; McKay, G. Pseudo-second order model for sorption processes. *Process Biochem.* **1999**, *34*, 451–465. [[CrossRef](#)]
45. McKay, G.; Poots, V.J.P. Kinetics and diffusion processes in colour removal from effluent using wood as an adsorbent. *J. Chem. Technol. Biot.* **1980**, *30*, 279–292. [[CrossRef](#)]
46. Weber, W.J.; Morris, J.C. Kinetics of adsorption on carbon from solution. *J. Sanit. Eng. Div. Am. Soc. Civ. Eng.* **1963**, *89*, 31–60. [[CrossRef](#)]
47. Mezenner, N.Y.; Bensmaili, A. Kinetics and thermodynamic study of phosphate adsorption on iron hydroxide-eggshell waste. *Chem. Eng. J.* **2009**, *147*, 87–96. [[CrossRef](#)]
48. Ellersdorfer, M. The ion-exchanger-loop-stripping process: Ammonium recovery from sludge liquor using NaCl-treated clinoptilolite and simultaneous air stripping. *Water Sci. Technol.* **2018**, *77*, 695–705. [[CrossRef](#)]
49. Li, M.; Zhu, X.; Zhu, F.; Ren, G.; Cao, G.; Song, L. Application of modified zeolite for ammonium removal from drinking water. *Desalination* **2011**, *271*, 295–300. [[CrossRef](#)]
50. Zhao, Y.; Zhang, B.; Zhang, X.; Wang, J.; Liu, J.; Chen, R. Preparation of highly ordered cubic NaA zeolite from halloysite mineral for adsorption of ammonium ions. *J. Hazard. Mater.* **2010**, *178*, 658–664. [[CrossRef](#)]